Steel and Composite Structures, *Vol. 35, No. 4 (2020) 509-525*
DOI: https://doi.org/10.12989/scs.2020.35.4.509

An innovative system to increase the longitudinal shear capacity of composite slabs

Rui Simões* and Miguel Pereira[a]

ISISE – Institute for Sustainability and Innovation in Structural Engineering; Department of Civil Engineering, University of Coimbra, Rua Luís Reis Santos – Polo II, 3030-788 Coimbra, Portugal

(*Received May 16, 2019, Revised April 25, 2020, Accepted April 30, 2020*)

Abstract. Steel-concrete composite slabs with profiled steel sheeting are widely used in the execution of floors in steel and composite buildings. The rapid construction process, the elimination of conventional replaceable shuttering and the reduction of temporary support are, in general, considered the main advantages of this structural system. In slabs with the spans currently used, the longitudinal shear resistance commonly provided by the embossments along the steel sheet tends to be the governing design mode. This paper presents an innovative reinforcing system that increases the longitudinal shear capacity of composite slabs. The system is constituted by a set of transversal reinforcing bars crossing longitudinal stiffeners executed along the upper flanges of the steel sheet profiles. This type of reinforcement takes advantage of the high bending resistance of the composite slabs and increases the slab's ductility. Two experimental programmes were carried out: a small-scale test programme – to study the resistance provided by the reinforcing system in detail – and a full-scale test programme to test simply supported and continuous composite slabs – to assess the efficacy of the proposed reinforcing system on the global behaviour of the slabs. Based on the results of the small-scale tests, an equation to predict the resistance provided by the proposed reinforcing system was established. The present study concludes that the resistance and the ductility of composite slabs using the reinforcing system proposed here are significantly increased.

Keywords: composite slab; longitudinal shear; reinforcing system; transversal bars; experimental tests

1. Introduction

Steel-concrete composite slabs are the most used structural systems for the conception of floors in steel or steel-concrete composite buildings. A steel-concrete composite slab, according to EN 1994-1-1 (CEN, 2004b), and, from now on, just referred to as by "composite slab", is a 2D structural component comprised of profiled steel sheeting in conjunction with a concrete layer placed above. In the definitive phase (composite action), the profiled steel sheet is used to resist tension stresses while the concrete is used to resist compressive stresses. In the construction phase, the profiled steel sheet is used as shuttering and is designed to resist the weight of the wet concrete plus the construction loads. This multi-functional role of the profiled steel sheeting leads to the main advantages of composite slabs, such as, the rapid construction process, the elimination of conventional replaceable shuttering and the reduction of temporary support.

The design of composite slabs submitted to uniform distributed loads for the ultimate limit states, as shown in Fig.1, may be governed by one of three failure modes: (i) the bending moment at the mid-span cross-section, (ii) the longitudinal shear along the shear span L_s or (iii) the vertical shear in a cross-section close to the supports. These three failure modes are represented in the graph shown in Fig. 1, which relates the maximum load p (defined by the vertical shear at the supports V_t) with the span length (defined by the shear span L_s); the remaining symbols in Fig. 1 have the following meanings: b is the width of the slab; d_p is the distance from the centroidal axis of the profiled steel sheeting to the upper top fiber of the composite slab in compression; A_p is the area of the cross-section of the profiled steel sheeting on the width b; L_s is the shear span length, equal to $L/4$ for a simple supported composite slab submitted to a uniform distributed load; m and k are constants regarding one of the methods (m-k method) given in standard EN 1994-1-1 (CEN, 2004b) to predict the longitudinal shear resistance of composite slabs. A composite slab failure induced by vertical shear is a predictable mode but only in short-span composite slabs. For current length spans between 2 and 5 m, the failure by longitudinal shear along the steel sheet-concrete interface is the most common type of failure, and consequently, the verification of the longitudinal shear resistance tends to be the governing design condition for this type of structural component. The bending moment resistance usually governs the design only in long-span slabs. The design may also be governed by the serviceability limit states, for composite slabs with low values of the relation h/L (thin slabs), where h is the slab's thickness and L is the span length. Taking the previous assumptions into account, increasing the longitudinal shear resistance seems to be one

*Corresponding author, Ph.D., Professor
E-mail: rads@dec.uc.pt
[a]Ph.D. Student
E-mail: mpereira@uc.pt

http://www.techno-press.org/?journal=scs&subpage=8
ISSN: 1229-9367 (Print), 1598-6233 (Online)

of the most effective ways to increase the load bearing capacity of composite slabs.

In Europe, the design of composite slabs is regulated by standard EN 1994-1-1 (CEN, 2004b), which states that the profiled steel sheeting must be capable of transmitting horizontal shear at the interface between itself and the concrete to ensure the composite behaviour. The composite behaviour between the two components (steel sheeting and concrete layer) must be ensured by one or more interlocking systems. As shown in Fig. 2, standard EN 1994-1-1 (CEN, 2004b) predicts 4 types of interlocking systems to be applied: (a) a mechanical interlock provided by indentations or embossments in the profile; (b) a frictional interlock; (c) an end anchorage provided by welded studs or another type of local connection between the concrete and the profiled steel sheeting, in combination with the previous ones; (d) an end anchorage system by deformation of the ribs at the end of the sheeting, which must be combined with a frictional interlock.

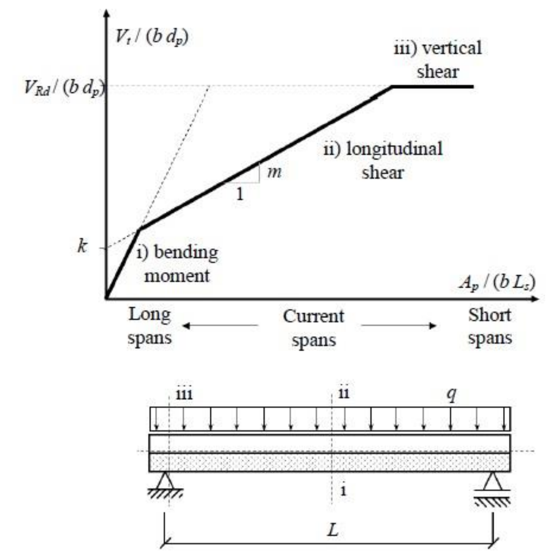

Fig. 1 Failure modes of composite slabs

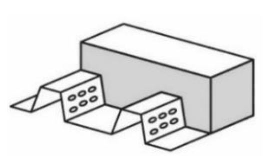

(a) Mechanical interlock

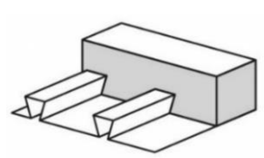

(b) Frictional interlock

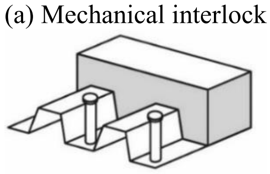

(c) End anchorage by welded studs

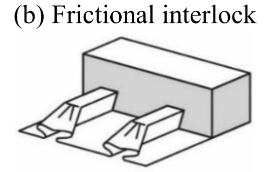

(d) End anchorage by deformation

Fig. 2 Typical forms of interlocking for composite slabs (CEN, 2004b)

According to standard EN 1994-1-1 (CEN, 2004b), the longitudinal shear resistance of a composite slab can be predicted by one of two methods: (i) the *m-k* method or (ii) the partial connection method. In general, the *m-k* method is quite conservative; it is based on empirical parameters obtained from slab tests meeting the basic requirements of the method and is valid for slabs with a brittle or ductile behaviour of the structural element. The partial connection method is also based on parameters obtained from tests but it allows us to take into account the contribution of any additional reinforcing system (e.g., end anchorage) or longitudinal reinforcing bars; however, its application is restricted to composite slabs with ductile behaviour.

To take better advantage of the high bending capacity of composite slabs, several researchers have been studying and developing different ways to improve the longitudinal shear behaviour of steel-concrete composite slabs. Some of these are reviewed in the following paragraphs.

Porter and Greimann (1984) carried out one of the first experimental studies to analyze the influence of end anchorage systems on steel-concrete composite slab resistance. These authors carried out an experimental programme comprising 15 prototypes of composite slabs with or without end anchorage devices constituted by end-span studs, in order to determine the percentage of load increase by comparing the prototypes without studs with the prototypes with studs. The test results showed that the inclusion of end studs increased the bearing load capacity of those composite slabs by 8 to 33%. Later, Jolly and Lawson (1992) studied the influence of end anchorage systems on composite slab behaviour; from the research work performed, they verified that the resistance of composite slabs with end anchorage devices almost doubled the resistance of composite slabs in comparison with those without any type of end anchorage device.

Chen (2003) tested 7 simply supported one-span and 2 continuous composite slabs with different end restraints to evaluate the influence of the shear bond action on the composite behaviour. The results obtained showed that the slabs with end anchorage were found to have a higher longitudinal shear bond resistance than the slabs without end anchorage. The author also noticed that the composite slabs without end anchorage devices showed a brittle behaviour, unlike those with end anchorage systems that showed a ductile behaviour.

Ferrer *et al.* (2006) carried out a numerical study to understand the effect of several geometrical aspects on the shear bond resistance, such as: the embossing slope, the sheet's thickness, the embossment depth, the profiling angle and the embossment inclination. The parametric study made it possible to optimize the slab's behaviour and to develop a new steel-sheet design method.

Chuan *et al.* (2008), in order to improve the longitudinal shear behaviour of composite slabs, performed an experimental programme to test composite slabs using shear screws to enhance the horizontal shear interaction. The results obtained showed that the shear screws increased the load carrying capacity and the ductility of the slab.

Some researchers (Salonikios, Sextos, & Kappos 2012; Saravanan, Marimuthu, Prabha, Arul Jayachandran, & Datta

2012) have been carrying out experimental programmes in accordance with standard EN 1994-1-1 (CEN, 2004b) to define the longitudinal shear resistance of composite slabs with specific steel sheet profiles. These authors tested 6 composite slabs for each profile to obtain the *m* and *k* values to allow the design of composite slabs for longitudinal shear using the *m*-*k* method in accordance with standard EN 1994-1-1 (CEN, 2004b).

Abas *et al.* (2013) studied the effect of steel fibres on steel-concrete continuous composite slabs. The researchers developed an experimental programme comprised by 8 two-span composite slabs with or without steel fibre reinforcement to study the influence of the quantity of steel fibre on the cracks that developed, on the redistribution of the bending moments, on the end slip and on the bearing capacity. The authors concluded that composite slabs containing a higher density of steel fibres achieved higher slip and peak loads.

Altoubat *et al.* (2015) evaluated the influence of fibres and welded-wire mesh reinforcements on the diaphragm behaviour of steel-concrete composite slabs. A set of twelve tests was carried out consisting of the application of a horizontal load on cantilever composite slabs. The slabs were supported by rollers on the side, the load was applied and fixed to a supporting steel beam on the opposite side. The specimens had different types of secondary reinforcement: varying the type (synthetic or steel) and dosage of the fibres or the type of the weld-wire mesh. The orientation of the specimens was also studied: eight slabs with the ribs perpendicular to the main beam and four slabs with ribs parallel to the main beam (strong and weak orientation, respectively, according to the authors). Two of the specimens (one for each direction) did not have any type of secondary reinforcement as a reference. The authors observed that slabs tested with a strong orientation developed a diagonal cracking pattern, while those with a weak orientation developed cracking in the thinner parts of the slab and achieved lower ultimate loads. The authors concluded that fibres increased the in-plane shear capacity by up to 50%, when compared to slabs without secondary reinforcement.

In the University of Coimbra, Fonseca *et al.* (2015), based on the study started by Carmona *et al*. (2009), improved the longitudinal shear resistance of composite slabs using transversal bars crossing the profiled steel sheeting at the middle height of the webs in the support cross-sections; this system behaves in a similar way to an end anchorage device constituted by welded studs (see Figs. 3(a) and 3(b)). The authors performed two experimental programmes: one small-scale specimen experimental programme to define an equation to determine the resistance provided by the new end anchorage system and one full-scale specimen experimental programme to analyze its influence on the behaviour of simply supported composite slabs. The second experimental programme comprised 8 tests of composite slabs with or without transversal bars in the support cross-sections and longitudinal bars on the concrete ribs. The failure mode of the specimens equipped with the end anchorage system was the bearing of the steel sheeting, as shown in Fig. 3(c). The results achieved showed that the proposed alternative end anchorage system increased the slab's capacity and ductility. However, the authors noted that the production of the steel sheet and the erection on site would be the main disadvantages of the system.

Rana *et al.* (2015a) carried out an experimental and numerical study to analyze the behaviour of composite slabs with and without end anchorage to reach a conclusion about the influence of this element on the bearing capacity and the failure mode of those slabs. The authors concluded that the

More recently, Ferrer *et al.* (2018) presented an innovative full-connection bonding mechanism, comprised of small crown-shaped cutting bands produced in the webs of the profiled steel sheeting as a replacement of the embossments, named the UPC-System and shown in Fig. 4. The researchers carried out an experimental campaign comprising several tests of composite slabs with three different commercial trapezoidal profiles, from 60 to 80 mm high and having the UPC-System or embossments on the profile's webs. The authors also tested different densities of punching (low, medium or high) and two different steel sheet thicknesses. The results showed that those slabs with the UPC-System achieved the full connection between the steel sheeting and concrete until the final failure without significant slip. The UPC-System also made it possible to increase the ultimate load.

Perfobond shear connectors are also a type of reinforcing system usually applied to improve the longitudinal shear behaviour of composite members, but mainly in steel-concrete composite beams. Nevertheless, Yang *et al.* (2018) studied the behaviour of steel-concrete composite slabs with flat horizontal steel sheeting and perfobond shear connectors – see Fig. 5.

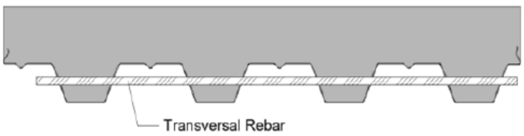

(a) Transversal cross-section

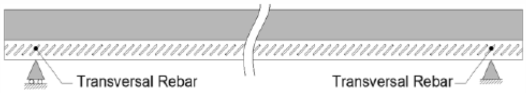

(b) Side view

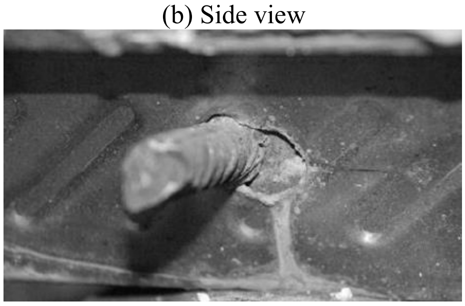

(c) Bearing of the steel sheeting

Fig. 3 End anchorage using transversal bars (Fonseca *et al.* 2015)

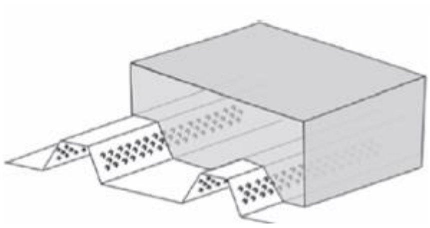

(a) System applied on slabs

(b) Crown-shaped cuttings

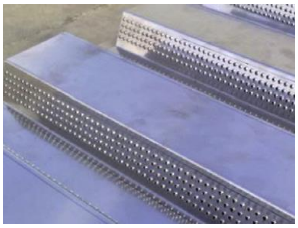

(c) Punched sheeting

Fig. 4 UPC System

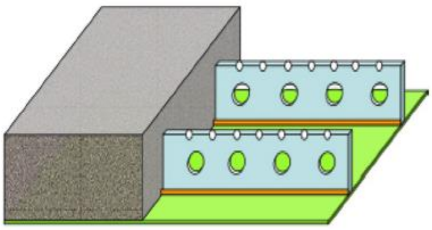

(a) Perfobond connectors in composite slabs

(b) Application in Donping bridge

(c) Specimen – steel part

Fig. 5 Perfobond connectors in composite slabs with flat steel sheeting

Flat steel sheeting saves money in moulding equipment and is easier to transport but also requires a greater thickness to compensate for the loss of bending stiffness when compared to profiled ones. Yang *et al.* (2018) tested two series of three composite slabs, each with flat steel sheeting and perfobond shear connectors. A thickness of 6 mm was used for the steel plates. The authors tested composite slabs with two different spans (3400 and 2400 mm for series 1 and 2, respectively) and three different amounts of transversal bars. All slabs failed by bending with yielding of the steel plate and the connectors. The authors concluded that full connection was achieved because no significant slip occurred between the steel plate and connectors and the concrete. The authors established a calculation approach based on the experimental results and validated it.

In order to overcome some of previously mentioned drawbacks concerning the behaviour of composite slabs, a research project (INOV_LAMI) was carried out at the University of Coimbra in a partnership between the Civil Engineering Department and a Portuguese steelwork company. The aim of the research project was to improve the behaviour of composite slabs, focusing on the development of an innovative reinforcing system to increase the longitudinal shear resistance along the steel sheet-concrete interface. This innovative system, described fully in this paper, was the object of a patent registration.

In the present paper the proposed innovative reinforcing system for longitudinal shear of composite slabs is presented. The system consists of a set of steel bars crossing longitudinal stiffeners executed along the upper flanges of the profiled steel sheeting. The reinforcing system is detailed in this paper, highlighting its versatility and main advantages. Two experimental test programmes were carried out: the first was comprised of an experimental programme of small-scale tests to determine the resistance of the reinforcing system and to calibrate an analytical expression to predict its design value; a second experimental campaign comprised a set of full-scale tests on simply supported and two-span continuous composite slabs. The results of the full-scale bending tests are compared with the resistance predicted, obtained according to the analytical procedures calibrated with the experimental results of the small-scale tests performed.

2. Proposed innovative reinforcing system for composite slabs

As explained before, the load bearing capacity of composite slabs is usually governed by the low degree of longitudinal shear connection ensured by the sheet embossments along the steel sheet-concrete interface. The end anchorage systems constituted by stud connectors welded to the flange of the supporting steel beams if welded through the steel sheet, are one of the most used ways to increase the degree of connection between the steel and the concrete. This reinforcing system is efficient; however, it has also some constraints: the welding of the stud connectors must be executed on the site, to be done through the steel sheet, and the supporting beam must preferably be a steel beam.

The reinforcing system developed and studied in the present research comprises a set of transversal reinforcing steel bars, distributed along the span, and placed in vertical cuts executed in the longitudinal stiffeners, for example in the inverted V-shape, located in the upper flanges of the profiled steel sheeting, as it is illustrated in Fig. 6(b). The function of the bars is to prevent the relative displacement between the profiled steel sheeting and the concrete in the longitudinal direction, allowing the slab to exercise its entire bending resistance. When demands are made on the system, the shear strength of the bars and the bearing strength of the sheet are mobilized. The transference of the longitudinal shear forces is all the more effective, the greater the thickness of the steel sheets is. To prevent the bars from loosening during concreting, these are fitted into a hole-shaped cut-out located at the base of the vertical cut, whose diameter, approximately equal to the diameter of the bar, may be slightly larger than the width of the cut, thus obtaining a snap fit between the bar and the profiled sheet.

Fig. 7 details the proposed reinforcing system, which could be applied in two different ways: (i) simple reinforcing system (Fig. 7(a)) consisted in just the transversal bars applied in the pre-drilled holes (Fig. 7(b)) or (ii) reinforcement mesh Fig. 7(c)) combining transversal and longitudinal bars. The latter could be prepared in such a way that the transversal bars, which only have a significant role in the region of the intersection with the longitudinal stiffeners, could be folded down to support the longitudinal bars and, consequently, replace the application of bar spacers, as shown in Fig. 7(d). Apart from these two ways of application, other variants may be used.

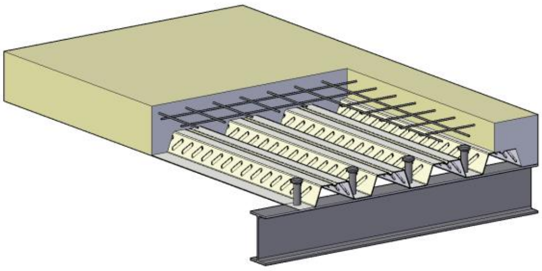

(a) End anchorage system of welded headed studs

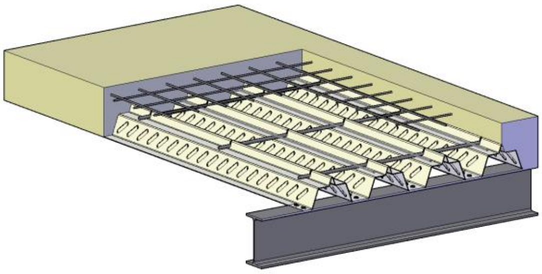

(b) Transversal reinforcing bars over the span

Fig. 6 Types of reinforcing systems for steel-concrete composite slabs

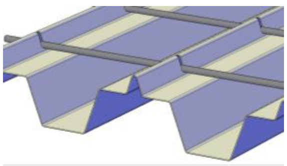

(a) Simple reinforcing system

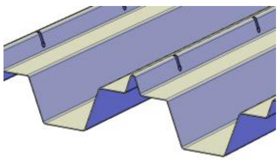

(b) Vertical cuts in the steel sheet

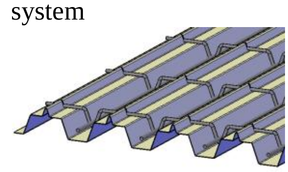

(c) Transversal and longitudinal bars

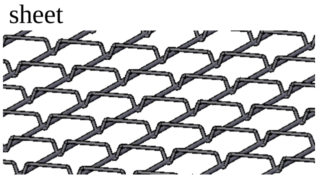

(d) Reinforcing mesh

Fig. 7 The reinforcing system developed

The proposed reinforcing system, developed to improve the longitudinal shear behaviour of composite slabs, has the following advantages, some of them obvious, others still to be proved by the results presented in the next sub-chapters: i) an increased load bearing capacity due to the increased longitudinal shear resistance; ii) for a given design loading scenario, the span of the slabs may be increased thereby decreasing the number of supporting beams required; iii) the system may be combined with the most common longitudinal shear resistant system constituted by embossments along the profiled steel sheeting; iv) easy to incorporate in the partial connection method, providing a less conservative design method for composite slabs when compared with the *m*-*k* method; v) the longitudinal shear capacity is no longer dependent on other possible reinforcing systems, such as the end anchorage device provided by headed studs welded to the supporting beams through the steel sheeting, which requires in-situ welding techniques; vi) the efficacy of the system does not depend on the material and shape of the supporting beams (e.g., timber or concrete beams may also be used as supporting beams); vii) increased ductility of the slabs because the most probable failure modes (bending or even longitudinal shear) are ductile; viii) increased transversal stiffness in the plane of the slab, which makes the diaphragm effect more effective, which is beneficial for resistance to horizontal actions, such as the action of the wind or the action of an earthquake; ix) support for the placement of other wire meshes (longitudinal and/or distribution) required for other functions; x) ease of on-site execution (cuts may be done previously in the factory). The possible leak of wet concrete (in the construction phase) through the gaps performed on the profiled steel sheeting to place the transversal bars can be avoided by closing the gaps, from the bottom side, with an expansive polyurethane foam or an adhesive tape.

In order to evaluate the efficiency of this reinforcing system by experimental tests, two new profile configurations were developed: (i) LAMI 60+ and (ii) LAMI 120+. The steel sheet profile LAMI 60+ was adapted from the profile H60, which has the dimensions specified on Fig. 8 and is already produced by the steelwork company involved in this research, for the purpose of the present study; the main difference between them consists in the longitudinal stiffener executed on the upper flange of the profile LAMI 60+ to fit the transversal bars on it. Fig. 9 shows the geometry of both the profiles developed, which were produced by folding and press braking processes, being all the geometric properties based on the full cross-section and not on the cross section at the notches; the geometric quantities specified are the height of the web h_p, the width of a module b_m, the mean width of a rib b_0, the vertical distance between the bottom flange and the position of the centroid of the steel sheet's cross-section e, the angle between the web and the horizontal plane φ, the width b_s and the height h_s of the longitudinal stiffener added on the upper flange. All the steel sheets used in the tests had a nominal thickness t_{nom} of 1.00 mm, and a core thickness of 0.96 mm after excluding the corrosion protection by hot-dip galvanizing, composed of two 0.02 mm thick layers on each face.

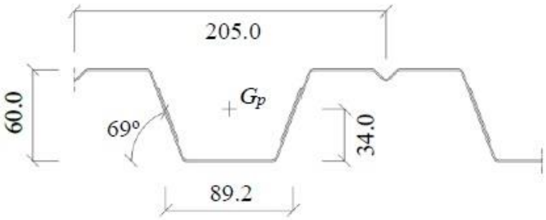

(a) H60 geometry

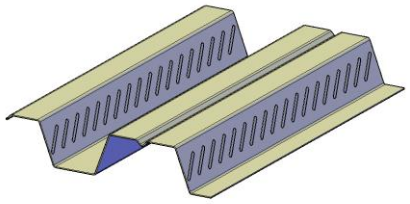

(b) H60 3D perspective

Fig. 8 The steel sheeting profile already produced (dimensions in mm)

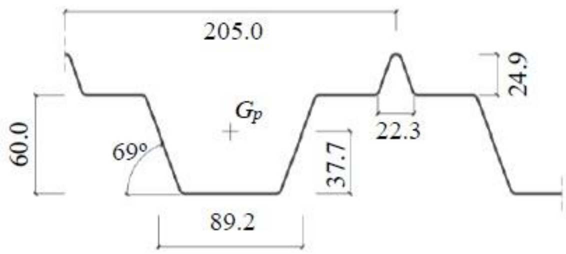

(a) LAMI 60+

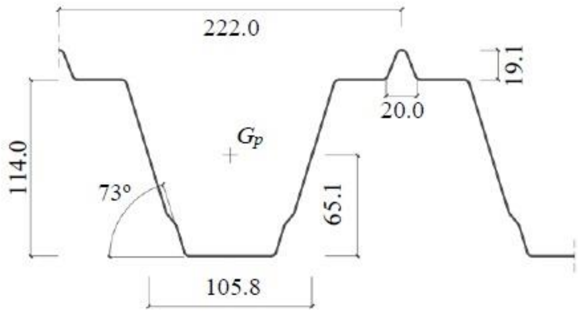

(b) LAMI 120+

Fig. 9 The steel sheeting profiles developed (dimensions in mm)

In accordance with the production process, the surface of the profiled steel sheeting used in the present research is smooth, without any type of embossments; as a consequence, it must be highlighted that once the adhesion connection is broken, the longitudinal shear resistance is entirely dependent on the bearing resistance of the transversal bars crossing the longitudinal stiffeners, which are the main components of the proposed reinforcing system.

Table 1 Main dimensions of the profiles used over this study

	h_w [mm]	b_m [mm]	b_0 [mm]	e [mm]	α [º]	b_s [mm]	h_s [mm]
H60	60.0	205.0	89.2	34.0	69	16.0	8.0
LAMI 60+	60.0	205.0	89.2	37.7	69	22.3	24.9
LAMI 120+	114.0	222.0	105.8	65.1	73	20.0	19.1

3. Evaluation of the resistance of the reinforcing system

3.1 Introduction

A small-scale experimental programme and a statistical analysis of the results were carried out to calibrate an equation to determine the bearing resistance of the transversal bars crossing the longitudinal stiffener produced along the upper flange of the profiled steel sheeting. The statistical analysis of the results was developed according to the standard evaluation procedure - method (a) - described in clause D8.2 of Annex D of standard EN 1990 (CEN, 2002), which requires, as the first step, developing a design model to obtain the theoretical resistance of the system. Then, to calibrate the design formula, a comparison procedure between the experimental and theoretical results must be made.

The behaviour of the transversal bars crossing the longitudinal stiffeners is similar to the bearing behaviour of a bolted shear connection. So, following the same procedure of Fonseca *et al.* (2015), the equation of the bearing resistance $F_{b,Rd}$ of a bolted shear connection (Eq. (1)), in accordance with Table 8.4 of standard EN 1993-1-3 (CEN, 2006), is selected as the basic equation to be calibrated in order to reproduce the equivalent phenomenon, relative to the transversal bars crossing the longitudinal stiffeners.

$$F_{b,Rd} = \frac{2.5\alpha_b k_t f_u d t}{\gamma_{M2}} \tag{1}$$

where:

- α_b is the minimum value between 1.0 and $e_1/(3d)$;
- e_1 is the distance to the end of the steel sheeting;
- d is the bar's diameter;
- k_t is given by $(0.8t+1.5)/2.5$ if $0.75\text{ mm} \leq t \leq 1.25\text{ mm}$ and by 1.0 if $t > 1.25$ mm;
- t is the thickness of the steel sheeting;
- f_u is the ultimate strength of the profiled steel sheeting;
- γ_{M2} is the partial safety factor with a recommended value of 1.25.

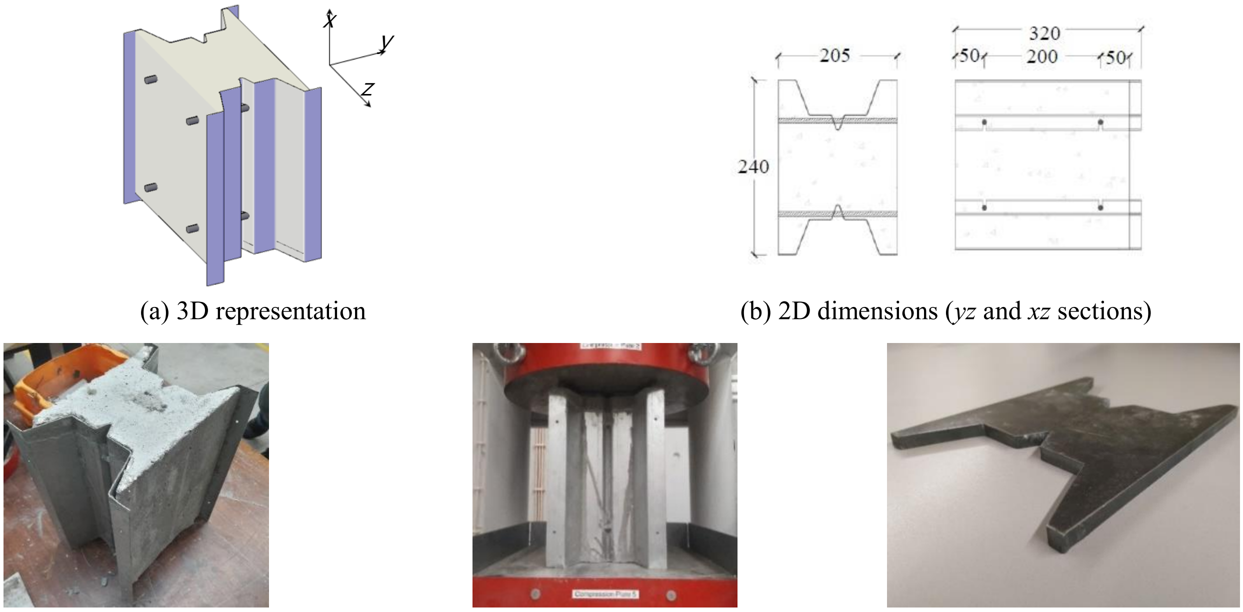

(a) 3D representation (b) 2D dimensions (yz and xz sections)

(c) Specimen example (d) Specimen compression (e) Steel plate for compression

Fig. 10 Experimental approach

3.2 Experimental approach

An experimental programme comprised of 15 specimens was carried out to determine the characteristic value of the resistance at each contact point between the transversal bars and the steel sheeting. Figs. 10(a) and 10(b) shows the geometry of the specimens tested. These specimens are constituted by a 300 mm long concrete part (in the direction of the load application - axis x), and two steel sheets, which are 20 mm longer to allow for the slip movement and consequently the transference of the applied load (by shear through the connecting bars) between the two different materials (steel and concrete). The cross-sections of the specimens (yz plane sections) were doubly symmetric to avoid eccentricity effects. Two reinforcing bars were placed crossing each steel sheet at a 50 mm distance from both end sections. Each specimen was loaded in compression along the x axis until its failure, using a 15 mm thick steel plate with a cross-section identical to the concrete part – Fig. 10(e). Tests were performed with displacement control: a displacement rate of 0.01 mm/s up to a total displacement of 2 mm, followed by a displacement speed of 0.02 mm/s until the failure. Five groups of three equal specimens were developed, as it is described in Table 2, varying: (i) the thickness of steel sheeting t – 0.8, 1.0 or 1.2 mm; the bar diameter d – 8 or 10 mm; the bar surface – smooth (S) or ribbed (R).

In order to quantify the concrete's resistance, uniaxial compressive tests were performed on cubic specimens with edges of 150 mm. To obtain the steel's tensile resistance, uniaxial tensile tests were performed on steel sheet specimens with a geometry according to standard ISO 6892-1 (ISO, 2009). The characterization of the concrete was carried out on the same day as the full-scale tests. An average compressive stress resistance f_{cm} of 40.41 MPa for the concrete and a corresponding characteristic value f_{ck} of 32.41 MPa, in accordance with EN 1992-1-1 (CEN, 2004a), were obtained; for the steel of the profiled steel sheets, an average yield stress f_{yp} of 329.51 MPa and an average ultimate stress f_{up} of 379.48 MPa were obtained. Regarding the reinforcing bars, average yield stresses f_{ys} of 598.37 MPa and 483.89 MPa were obtained for bars with diameters of 8 and 10 mm, respectively.

Fig. 11(a) shows the P-s curves obtained for one of each type of specimen, where P is the applied load and s is the measured slip. From this graph it is possible to conclude that the bearing capacity is higher for thicker steel sheets and larger bar diameters, as expected. The ductility of the reinforcing system is also higher for the thicker steel sheets. These observations were already expected and were in accordance with conclusions obtained by Fonseca *et al.* (2015), based on the small scale test campaign carried out. Fig. 11(b) represents, for exemplification, P-s curves for the three specimens of the SS_1.0_8R group. Table 2 presents the peak load values obtained in each group of tests, and also the corresponding average values.

3.3 Statistical analysis

Annex D from standard EN 1990 (CEN, 2002) provides guidance to develop design procedures assisted by testing. In order to calibrate an equation to predict the resistance of the reinforcing system (at each contact point), a statistical analysis of the experimental results obtained was performed as presented hereafter. The statistical analysis of the results was developed according to the method (a) of Annex D of standard EN 1990 (CEN, 2002), consisting in a 7 step method to define a characteristic resistance value.

Table 2 Experimental specimens tested and results – small-scale tests

Specimen Type	t [mm]	d [mm]	Bar surface	P_i [kN]			P_m [kN]
SS_0.8_8R	0.8	8	Ribbed (R)	58.50	52.10	52.20	54.27
SS_1.0_8R	1.0	8	Ribbed (R)	68.90	69.90	71.20	70.00
SS_1.2_8R	1.2	8	Ribbed (R)	65.50	67.40	71.70	68.20
SS_1.2_8S	1.2	8	Smooth (S)	88.50	84.30	68.60	80.47
SS_1.2_10R	1.2	10	Ribbed (R)	89.80	76.60	106.30	90.90

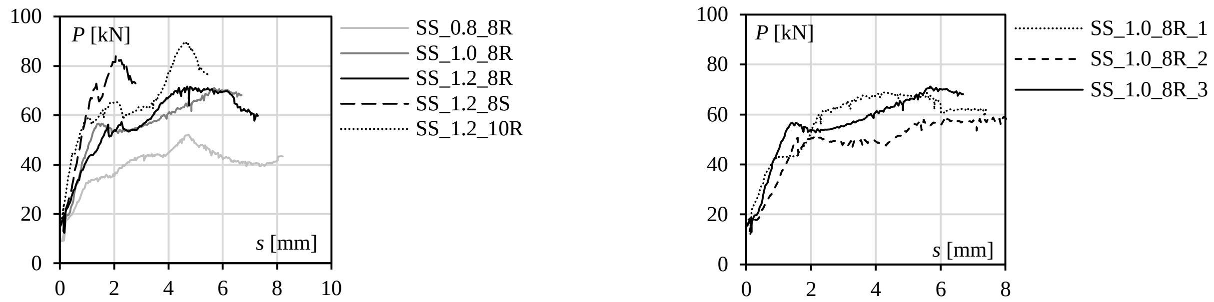

(a) P-s curve for each specimen type (b) P-s curves for SS_1.0_8R specimens

Fig. 11 Experimental results

The design model defined by Eq. (1) (bearing resistance in a bolted shear connection) was chosen to define the theoretical values for the resistance of the reinforcing system, at each contact point. For current situations – thickness of the steel sheet between 0.75 and 1.50 mm and bar diameters higher than 8 mm – the shear resistance of the reinforcing bar does not need to be taken in account because the resistance of the system is governed by the bearing capacity of the steel sheet. Table 3 presents the determination of the theoretical resistance r_{ti} for a contact point for each group of specimens, obtained using the Eq. (1) and the real material properties; taking into account the negligible differences between the real and the nominal geometric properties observed in the tests, for simplification the latter were used.

After defining the theoretical values for the contact point resistances, these values should be compared with the experimental results. Fig. 12 presents a plot with all pairs of corresponding values (r_{ti}, r_{ei}), where r_{ei} corresponds to the experimental resistance given by one eighth of the peak load (values P_i in Table 2) obtained experimentally ($X_i/8$). The value obtained for the mean value correction factor b was 1.1323 and it represents the "least squares" best fit to the slope represented on the graph. Error term δ_i for each r_{ei} value was defined through Eq. (3); the coefficient of variation V_δ is defined by Eq. (7)

$$b = \frac{\sum_{i=1}^{n} r_{ei} r_{ti}}{\sum_{i=1}^{n} r_{ti}^2} \tag{2}$$

$$\delta_i = \frac{r_{ei}}{b \cdot r_{ti}} \tag{3}$$

$$\Delta_i = \ln(\delta_i) \tag{4}$$

$$\bar{\Delta} = \frac{1}{n} \sum_{i=1}^{n} \Delta_i \tag{5}$$

$$s_\Delta^2 = \frac{1}{n-1} \sum_{i=1}^{n} \left(\Delta_i - \bar{\Delta}\right)^2 \tag{6}$$

$$V_\delta = \sqrt{\exp\left(s_\Delta^2\right) - 1} \tag{7}$$

where:

δ_i	is the error term for specimen i;
Δ_i	is the logarithm of the error term δ_i;
$\bar{\Delta}$	is the estimated value for $E(\Delta)$;
s_Δ	is the standard deviation of Δ_i values;
V_δ	is the coefficient of variation of error terms δ_i.

The ultimate tensile strength of the steel sheet f_{up} is the only basic variable included in the initial design model (geometrical parameters have been considered deterministically). The coefficient of variation of this variable was found to be 0.06 as shown in Table 4. This value was compared with previous studies from the bibliography and similar values for this coefficient were found (Simões da Silva *et al.* 2009; Simões da Silva *et al.* 2018). The coefficients of variations V_{rt} and V_r must be

Table 3 Theoretical resistance values r_{ti}

Specimen type	t [mm]	t_{cor} [mm]	d [mm]	α_b	k_t	f_u [MPa]	γ_{M2}	r_{ti}
SS_0.8_8R	0.8	0.76	8	1.00	0.84	379.48	1.00	4.86
SS_1.0_8R	1.0	0.96	8	1.00	0.91	379.48	1.00	6.61
SS_1.2_8R	1.2	1.16	8	1.00	0.97	379.48	1.00	8.55
SS_1.2_8S	1.2	1.16	8	1.00	0.97	379.48	1.00	8.55
SS_1.2_10R	1.2	1.16	10	1.00	0.97	379.48	1.00	10.69

Table 4 Determination of the coefficient of variation of the ultimate strength f_{up}

Basic variable	$x_{k,i}$	m_x	s_x^2	s_x	$V_{Xi} = s_x / m_x$
	354.72				
f_{up} [MPa]	383.68	379.476	526.228	22.940	0.060
	400.02				

obtained and, for small values of V_δ^2 and V_{Xi}^2, these values could be obtained according to Eqs. (8) and (9), respectively. Using the Eqs. (7)-(9), numerical values for the coefficients of variation $V_{\square}$, V_{rt} and V_r of 0.159, 0.060 and 0.170, respectively, were obtained.

$$V_{rt} = \sqrt{\sum_{i=1}^{j} V_{Xi}^2} \tag{8}$$

$$V_r = \sqrt{V_\delta^2 + V_{rt}^2} \tag{9}$$

where V_{Xi} is the coefficient of variation of the basic variable X.

The characteristic resistance value r_k should be obtained from Eq. (10). And so, the calibration factor η to apply to the original design model is defined according to Eq. (11).

$$r_k = b \cdot g_{rt}\left(\underline{X}_m\right)\exp\left(-k_\infty \alpha_{rt} Q_{rt} - k_n \alpha_\delta - 0.5Q^2\right) \tag{10}$$

$$\eta = b \cdot \exp\left(-k_\infty \alpha_{rt} Q_{rt} - k_n \alpha_\delta - 0.5Q^2\right) \tag{11}$$

where

$$Q_{rt} = \sqrt{\ln\left(V_{rt}^2 + 1\right)} \tag{12}$$

$$Q_\delta = \sqrt{\ln\left(V_\delta^2 + 1\right)} \tag{13}$$

$$Q = \sqrt{\ln\left(V_r^2 + 1\right)} \tag{14}$$

$$\alpha_{rt} = \frac{Q_{rt}}{Q} \tag{15}$$

$$\alpha_\delta = \frac{Q_\delta}{Q} \tag{16}$$

and k_∞ and k_n are the fractile factors given by 1.64 and 1.84, respectively, for a number of experiments $n = 15$ and considering V_X unknown, according to Table D.1 of Annex D from standard EN 1990 (CEN, 2002).

Developing this procedure, a calibration factor of 0.8205 for η was found and the longitudinal shear resistance at each contact point (between the transversal bar and steel sheet) $F_{t,Rd}$ should be defined as expressed in Eq. (17) in the design stage. Considering the transversal bars uniformly distributed along the span and two contact points on each inverted V-shape stiffener, the resistance to longitudinal shear can be defined as a resistant force per unit of area, so a resistant stress $\tau_{t,Rd}$ given by Eq. (18). Fig. 12 shows the diagram of every pair obtained $F_{b,Rd} - F_{t,Rd}$, with the respective best-fit linear function with a b slope, and the comparison of these with the design equation developed. All pairs r_{ti}-r_{te} are above this line so it could be assumed that the equation developed may adequately represent a design model for the proposed reinforcing system.

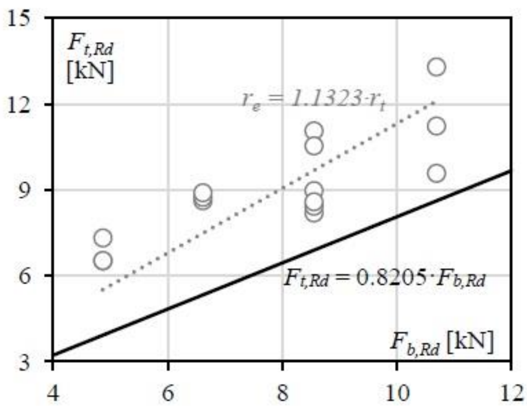

Fig. 12 Diagram $F_{t,Rd} - F_{b,Rd}$

$$F_{t,Rd} = 0.8205 \frac{2.5\alpha_b k_t f_u dt}{\gamma_{M2}} \tag{17}$$

$$\tau_{t,Rd} = \frac{2F_{t,Rd}}{b_m l_b} = 4.103 \frac{\alpha_b k_t f_u dt}{b_m l \gamma_{M2}} \tag{18}$$

where:

b_m is the width of a composite slab module;

l_b is the length between the transversal bars.

3.4 Design of composite slabs reinforced with the proposed system

Based on the experimental results presented in the next sub-chapter, a composite slab reinforced with transversal bars according to the reinforcing system proposed in the scope of the present paper has a ductile behaviour. So, the partial connection method can be used to predict its bending and longitudinal shear resistance. The application of such methodology, already incorporating the contribution of the proposed reinforcing system, is described hereafter.

According to standard EN 1994-1-1 (CEN, 2004b), if the partial connection method is used it should be shown that at any cross-section the design bending moment M_{Ed} must be lower than the design resistance M_{Rd}. The design resistance M_{Rd} for unit of width b (in general the slab module b_m) should be determined by Eq. (25), according to the stress diagrams shown in Fig. 13. For composite slabs with transversal bars crossing the profiled steel sheeting, the design shear strength $\tau_{u,Rd}$ should be replaced by $\tau_{t,Rd}$ evaluated according to Eq. (18).

$$N_p = A_{pe} f_{yp,d} \tag{19}$$

$$N_{cf} = \min\left\{N_p ; 0.85 f_{cd} b h_c\right\} \tag{20}$$

$$N_c = \tau_{u,Rd} b L_x \leq N_{cf} \tag{21}$$

$$z_{pl} = \frac{N_c}{0.85 f_{cd} b} \tag{22}$$

$$z = h - \frac{z_{pl}}{2} - e_p + \left(e_p - e\right)\frac{N_c}{N_p} \tag{23}$$

$$M_{pr} = 1.25 M_{pa}\left(1 - \frac{N_c}{A_{pe} f_{yp,d}}\right) \leq M_{pa} \tag{24}$$

$$M_{Rd} = N_c z + M_{pr} \tag{25}$$

where:

N_c is the compressive force in the concrete, defined according to Eq. (21);

M_{pr} is the reduced plastic resistant moment of the profiled steel sheeting;

$\tau_{u,Rd}$ is the design shear strength (to be replaced by $\tau_{t,Rd}$ given by Eq. (18));

L_x is the distance of the cross-section being considered to the nearest support;

N_{cf} is the compressive force in the concrete for full shear connection;

N_p is the tensile force in the profiled steel sheeting;

f_{cd} is the design value of the compressive strength of the concrete;

$f_{yp,d}$ is the design value of the tensile strength of the steel of the profiled sheet;

z_{pl} is the distance between the plastic neutral axis and the upper surface of the slab;

e_p is the distance between the plastic neutral axis and the lower flange of the profiled steel sheeting;

e is the distance between the centroidal axis and the lower flange of the profiled steel sheeting;

A_{pe} is the effective cross-section area of the profiled steel sheeting;

M_{pa} is the design value of the plastic resistant bending moment of the effective cross-section of the profiled steel sheeting.

Other symbols are represented in Fig. 13 or explained before.

If, in addition to the proposed reinforcing system, longitudinal reinforcing bars are to be used on the concrete ribs, the previous formulation must be adapted in accordance, which may be consulted elsewhere (Fonseca *et al.* 2015, Johnson and Shepherd 2013).

4. Experimental verification of the efficacy of the proposed reinforcing system

4.1 Introduction

An experimental campaign was carried out to evaluate the efficacy of the proposed reinforcing system on the global behaviour of simply supported and continuous composite slabs. Fig. 14 shows the specimens in production and composite phases. The experimental results obtained in this experimental campaign were also used to verify the accuracy of the design methodology presented in the previous sub-chapter, the partial connection method of standard EN 1994-1-1 (CEN 2004b), accounting for the longitudinal shear strength through Eq. (18).

In order to characterize the concrete, uniaxial compressive tests were performed on cubic specimens with edges of 150 mm. To obtain the steel's tensile resistance, uniaxial tensile tests were performed on steel sheet specimens with a geometry according to standard ISO 6892-1 (ISO 2009). The characterization of the material was carried out in the same week as the full-scale tests. An average compressive stress resistance f_{cm} of 36.32 MPa for the concrete and a corresponding characteristic value f_{ck} of 28.32 MPa, in accordance with Eurocode 2 (CEN 2004a), was obtained; for the steel of the profiled sheets, average yield stresses f_{yp} of 329.51 MPa (LAMI 60+), 363.57 MPa (LAMI 120+) and 388.73 MPa (H60) were obtained.

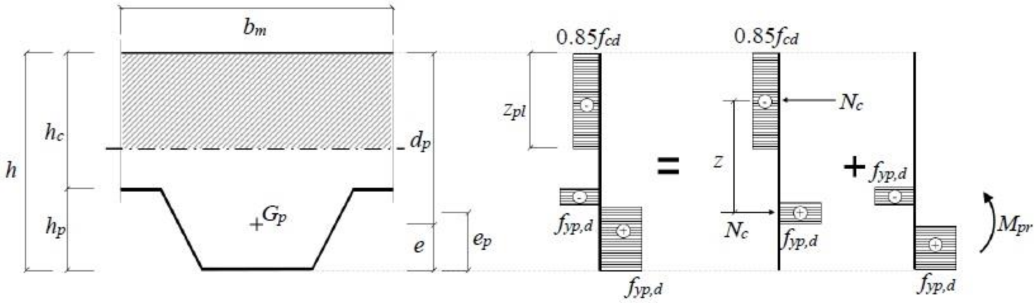

Fig. 13 Stress distribution for the sagging bending resistance of a composite slab

(a) Reinforcing system

(b) Specimens for simply supported slabs

(c) Specimens for continuous slabs

Fig. 14 Specimen preparation

Regarding the reinforcing bars, average yield stresses f_{ys} of 598.37 MPa, 483.89 MPa and 476.89 MPa were obtained for bars with diameters of 8, 10 and 12 mm, respectively.

4.2 Experimental programme

The second experimental programme carried out for the present research work consisted of 6 experimental full-scale tests, divided into two groups: one group of simply supported slabs – group A and another group constituted by 2 span continuous slabs – group B. Group A comprised four bending tests of simply supported composite slabs with 2.8 m span lengths L. These slabs were loaded with four transversal linear loads applied symmetrically in relation to the half span cross-section and spaced by $L/4$, as shown in Fig.15. This loading system was established in order to approximate as much as possible a real loading scenario, which, in general, is constituted by a uniformly distributed load. Fig. 16 shows the cross-section of each specimen from test group A, specifying the reinforcement bars applied. Group B comprised two bending tests on continuous slabs with 2 equal spans of 2.8 m in length. These slabs were also loaded with four linear transversal loads applied symmetrically to the intermediate support section, as shown in Fig. 17. Fig. 18 shows the cross-section of each specimen from test group B, specifying the reinforcement bars applied.

The effect of the transversal bars crossing the profiled steel sheeting was studied for slabs with LAMI 60+ (A_1 and A_2) or LAMI 120+ (A_3 and A_4) profiles in group A. In all specimens of this group, 8 mm diameter transversal barswere uniformly distributed over the span, with a space of 200 mm between them. Specimens A_1 and A_2 were identical, although the surface roughness of the bars used was different: bars with a smooth (S) surface in specimen A_1 and bars with a ribbed (R) surface in specimen A_2.

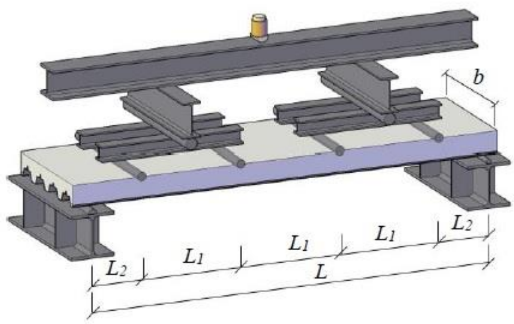

Test	A_1	A_2	A_3	A_4
b	820	820	666	666
h	150	150	200	200
h_p	60.0	60.0	113.96	113.96
h_c	90	90	86.04	86.04
L	2800	2800	2800	2800
L_1	700	700	700	700
L_2	350	350	350	350

Fig. 15 Experiment layout (dimensions in mm) – Group A

Specimens A_3 and A_4 were also identical, but the specimen A_4 had 2 additional longitudinal bars, one in each concrete rib. The lateral flanges of the profiled steel sheeting were bended in order to avoid local buckling and ensure the transversal continuity of the slabs.

The specimens from group B were identical, except for the longitudinal shear reinforcing system: specimen B_1 was constituted by an H60 profiled steel sheeting without any type of longitudinal shear reinforcement, therefore the longitudinal shear resistance was acquired only from the embossments on the profile (a base case) and; specimen B_2 was constituted by a LAMI 60+ profiled steel sheeting, reinforced with 10 mm diameter transversal bars uniformly distributed over the slabs, crossing the longitudinal stiffeners with a space of 400 mm between them (a specimen with the proposed reinforcing system). In the region of the intermediate support, 12 mm diameter longitudinal bars were placed with a space of 150 mm between them in both specimens; the coverings, measured from the centroids of the longitudinal bars and the top concrete surface was of 30 mm.

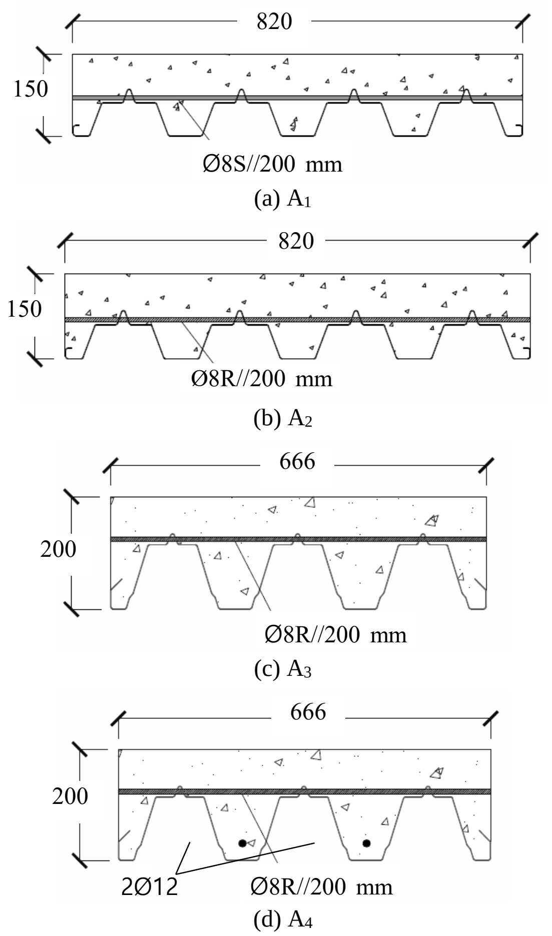

Fig. 16 Cross-section of the specimens – Group A

The tests were carried out applying an increasing load, controlled by a displacement increase of 0.02 mm/s until the plastic behaviour was reached and 0.04 mm/s in a subsequent phase until failure. Fig. 19 shows the instrumentation prepared for tests from groups A (Fig. 19(a)) and B (Fig. 19(b)). In all the specimens, strain gauges (SG) were applied on the steel sheeting. These strain gauges were placed at the bottom flange of the middle rib on cross-sections A and B, respectively for specimens from groups A and B, according to Fig. 19. Load cells (LC) were used on the supports and on the loading system to measure the reaction forces and the load applied. Several displacement transducers (LVDTs) were also used to measure the deflections along the span and the slip between the steel and the concrete at both ends. The deflection results presented on the next section were considered to be the values obtained from LVDTs 2 and 3, for tests from group A, and from LVDTs 1 and 2, for tests from group B.

4.3 Experimental results

4.3.1 Group A – simply supported slabs

All the slabs of the present group reached failure by longitudinal shear, but for a loading level close to the bending moment capacity. In all the specimens tensile cracks developed in the concrete in the tension zone of the slab's cross-section, along the span length with uniform bending moment (close to the mid span) (see Fig. 20(a)). The longitudinal shear failure was governed by the bearing of the steel sheeting, as shown in Fig. 20 (b).

Fig. 21 shows the results obtained for the test specimens in group A. P-δ, P-s and P-ε curves are represented in Figs. 21(a)-21(c), respectively, where: P is the total applied load, δ is the mid-span section's vertical deflection, s is the slip measured at one of the slab's extremities and ε is the maximum strain measured at the bottom flange of the steel sheet in the mid-span cross-section.

Experimental tests A_1 and A_2 showed a similar general behaviour. However, the peak load achieved on test A_1 was slightly higher than the one achieved on test A_2. No significant effects were observed due to the difference in the surface roughness of the transversal bars used; this difference is due to the common dispersion of results on experimental programmes. The use of longitudinal reinforcing bars significantly increased the resistance of the composite slab, which can be verified from the comparison of the test results of specimens A_3 and A_4; the maximum load achieved increased 34.56% from specimen A_3 to specimen A_4 just with 2 additional longitudinal bars. The greater thickness of the slabs of specimens A_3 and A_4 results in a larger bending stiffness as expected. Generally, all the specimens showed a high resistance and high ductility; the low values of the end slips measured at both ends (see Fig. 21(b)) allow us to conclude that the incorporation of the transversal bars crossing the profiled steel sheeting makes it possible to reach high degrees of longitudinal shear connection. The maximum strains measured at the bottom flange of the steel sheet in the mid-span cross-sections of all the specimens were also much higher than the yield strain of the steel used ε_{yp} (see Fig. 21(c)), which means that the

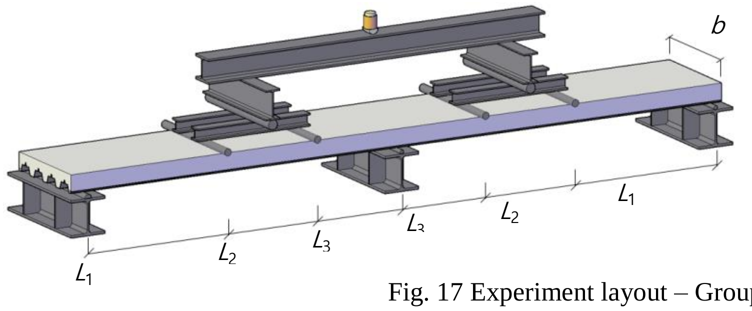

b =	820 mm
h =	150 mm
h_p =	60 mm
h_c =	90 mm
L =	2800 mm
L_1 =	1250 mm
L_2 =	800 mm
L_3 =	750 mm

Fig. 17 Experiment layout – Group B

(a) B_1 (b) B_2

Fig. 18 Cross-section of the specimens – Group B

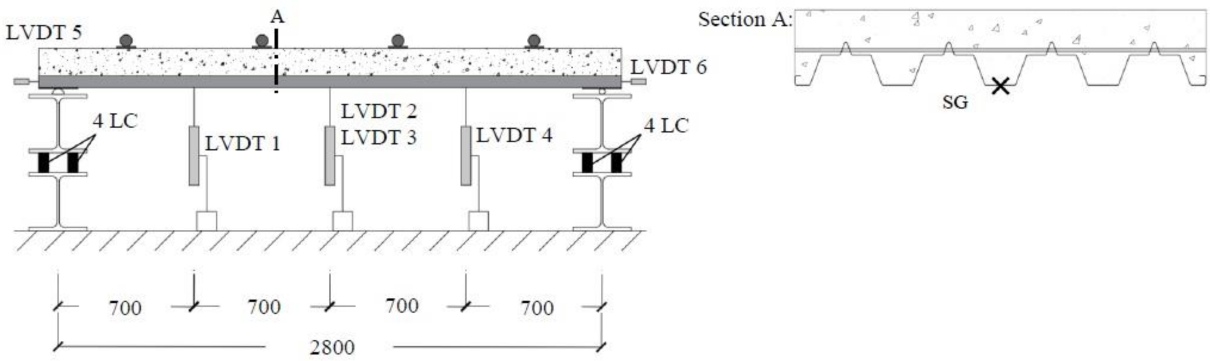

(a) Group A

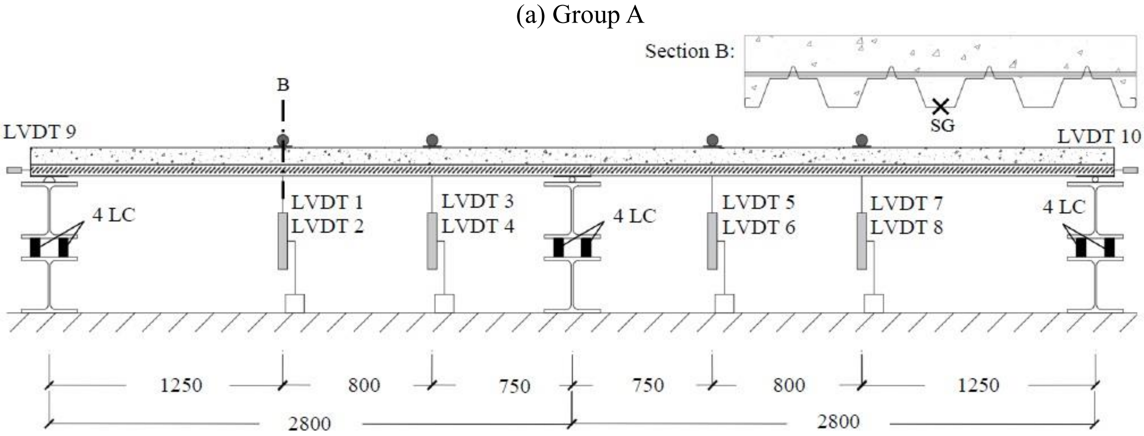

(b) Group B

Fig. 19 Instrumentation of experimental tests

plastic bending capacity of the slabs tested was almost attained.

For each test, Figs. 22(a)-22(d) shows: (i) the sagging bending moment measured along the span – M_{Test}; (ii) the sagging bending moment resistance of the slab's cross-

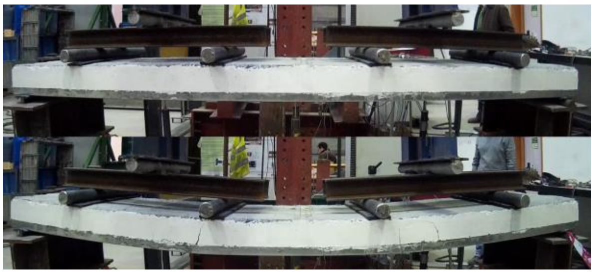

(a) Experimental test set-up

(b) Bearing of the steel sheet

(c) Slip at the ends

(d) Crack pattern at the mid-span

Fig. 20 Experimental approach

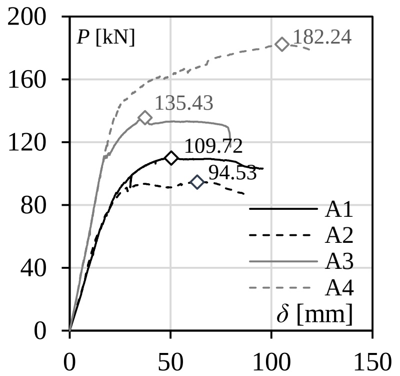

(a) P-δ curves

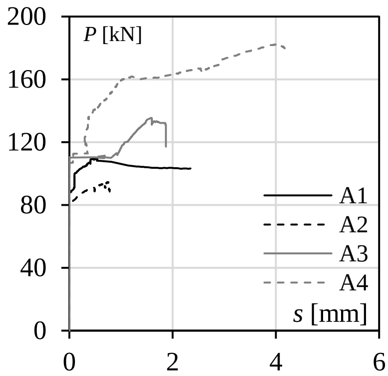

(b) P-s curves

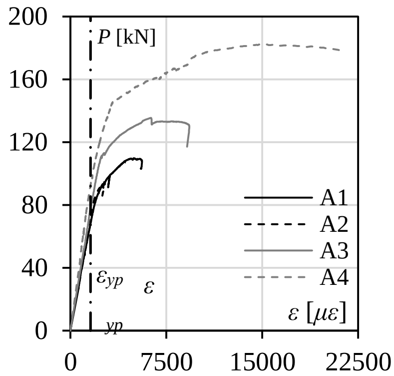

(c) P-ε curves

Fig. 21 Experimental results – Group A

section – bending moment resistance of the slab's cross-section – $M_{pl,Rd}$; (iii) the sagging bending moment resistance according to the partial connection method predicted in standard EN 1994-1-1 (CEN 2004b), already incorporating the proposed reinforcing system - M_{Rd}; (iv) the sagging bending moment expected along the span, if governed by the longitudinal shear resistance – M_{Ed}. The analytical values were evaluated using the average mechanical properties (real properties) of the materials instead of the design values. In tests A_1, A_2, A_3 and A_4 the maximum sagging bending moments measured M_{Test} were 36.99%, 17.94%, 27.90% and 11.51% higher respectively than the maximum bending moments that were expected M_{Ed}. Furthermore, the maximum sagging bending moment measured M_{Test} in test A_1 was 8.23% higher than the plastic moment resistance $M_{pl,Rd}$; in the remaining tests, lower values were reached although they were always very close to the plastic bending resistance of the slab's cross-section.

The results obtained in this group of tests allow us to conclude that: (i) the proposed reinforcing system constituted by transversal bars crossing the profiled steel sheeting, if adequately designed, allows the full bending capacity of a composite slab to be reached and; (ii) the design methodology based on the partial connection method, incorporating the longitudinal shear strength acquired by the proposed reinforcing system, can be used to predict the resistance of a composite slab.

4.3.2 Group B – continuous slabs

Test group B was developed to verify the efficacy of the proposed reinforcing system when applied in continuous composite slabs. Both specimens collapsed by longitudinal shear, as it is shown on Fig. 23. Fig. 24 shows the similar results obtained for the tests on group B. P-δ, P-s and P-ε

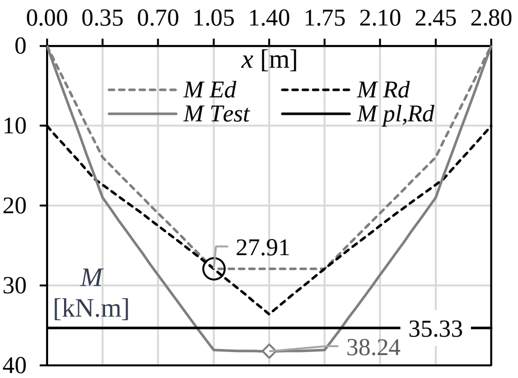

(a) A_1

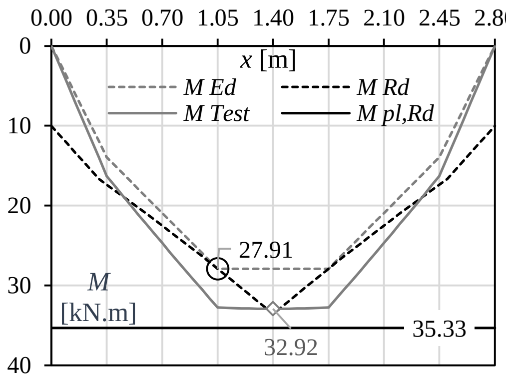

(b) A_2

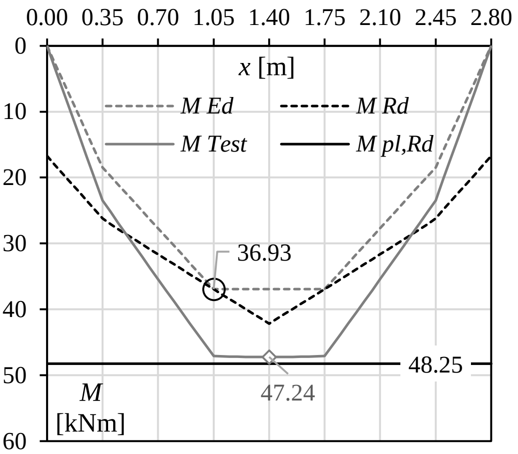

(c) A_3

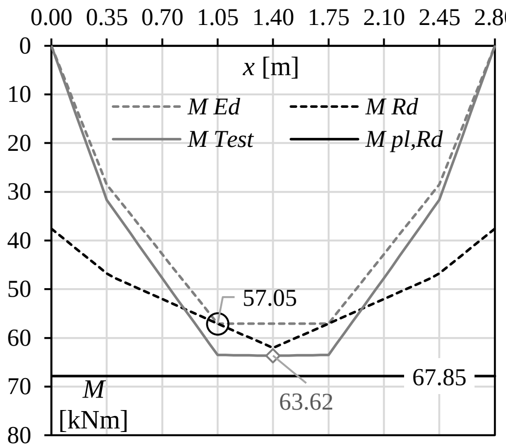

(d) A_4

Fig. 22 Bending moment diagrams – Group A

(a) Longitudinal shear B_1

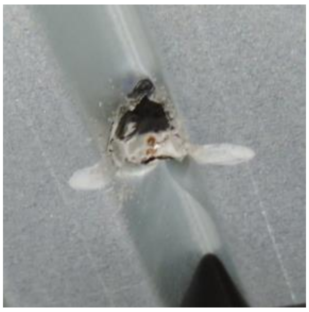

(b) Longitudinal shear B_2

(c) Experimental test B_2

Fig. 23 Failure of specimens from group B

curves are represented in Figs. 24(a)-24(c) respectively. Based on the results obtained and taking into account that the geometry of both profiles were similar, an increase of 43.03 % was observed in the maximum load achieved caused by replacing the embossments in the steel sheet profile (test B_1) with the transversal bars crossing the longitudinal stiffener (test B_2). Furthermore, the ductility acquired was significant. In test B_1 a brittle behaviour was obtained, since the slip started immediately after the maximum load level was reached, while in test B_2, the load significantly increased even after the first slip. The slip developed in test B_1 was also significantly higher, when compared with the one in test B_2.

Following the same procedure used for group A, Fig. 25 presents the bending moment diagrams M_{Test}, $M_{pl,Rd}$ along the span and M_{Rd} and M_{Ed} for test B_2. Since specimen B_1 presented a brittle behaviour according to standard EN 1994-1-1 classification, the partial connection method must not be applied to evaluate its resistance to longitudinal shear.

The results of group B show that the proposed reinforcing system makes it possible to significantly increase the ductility of steel-concrete composite slabs. The bending moment diagram M_{Test} obtained in test B_2, compared with the predicted diagram M_{Ed} according to the methodology proposed in the previous chapter, was very accurate.

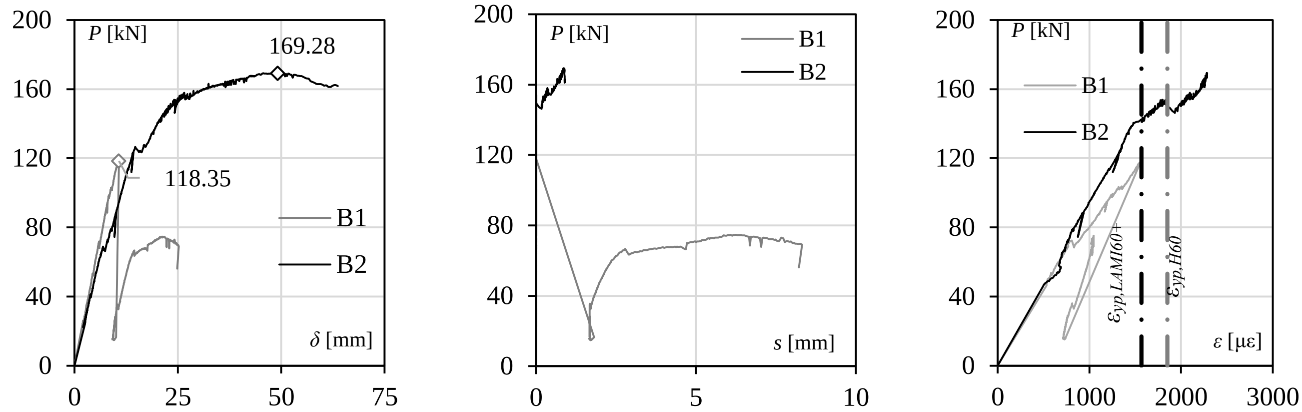

(a) *P-δ* curves (b) *P-s* curves (c) *P-ε* curves

Fig. 24 Experimental results – Group B

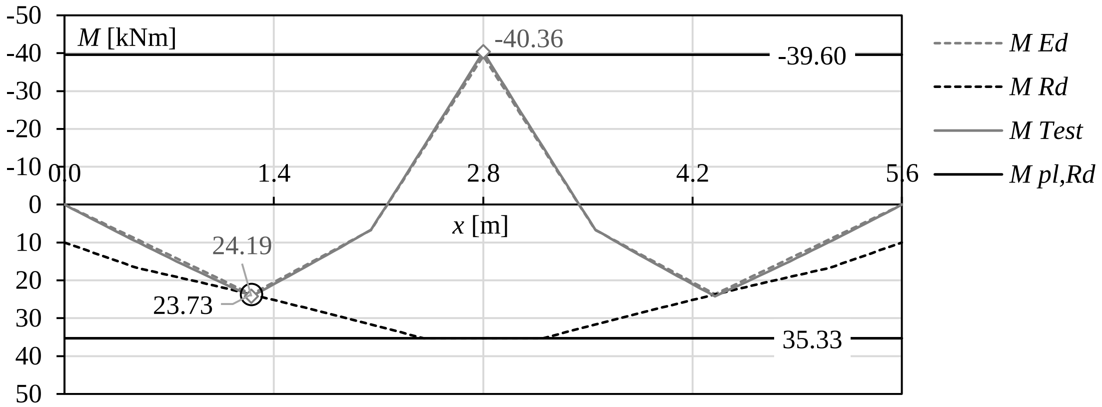

Fig. 25 Bending moment diagrams – Test B_2

5. Conclusions

In the scope of a research project carried out in the University of Coimbra, in a partnership between the Civil Engineering Department and a Portuguese steelwork company, an innovative reinforcing system for steel-concrete composite slabs was proposed and studied experimentally. The reinforcing system consists in transversal bars uniformly distributed over the span, crossing longitudinal stiffeners executed on the upper flange of the profiled steel sheeting, which allows to improve the behaviour of steel-concrete composite slabs. Some of the advantages are obvious taking into account just the mode of the reinforcing system:

- with the proposed reinforcing system, the slab’s behaviour is independent of end anchorage devices, which are normally dependent on the way the slab is supported and the material and shape of the supporting beams;
- if the transversal bars are continuous along the perpendicular direction of the ribs of profiled steel sheeting, the transversal stiffness in the plane of the slab is increased, which makes the diaphragm effect more effective;
- the proposed reinforcing system could be combined with the most common longitudinal shear resistant system constituted by embossments along the profiled steel sheeting, although this needs to be confirmed through additional research.

Based on the test results and their analyses presented throughout this paper, a summary of the main conclusions is:

- the reinforcing system proposed, developed to increase the longitudinal shear capacity, allows the full bending capacity of a composite slab to be reached and provides high levels of ductility, if adequately designed;
- taking into account the bearing failure mode at the contact points between the transversal bars and the steel sheets, the proposed reinforcing system is all the more effective the greater the thickness of the steel sheets;
- the design methodology based on the partial connection method, incorporating the longitudinal shear strength acquired by the proposed reinforcing system may be used to predict the resistance of a composite slab.

Acknowledgments

The authors would like to thank the team from the Laboratory of Structures of the Department of Civil

Engineering of the University of Coimbra. Thanks and recognition are also given to the Portuguese steelwork company O Feliz Metalomecânica SA, the partner in the research project, for the production of the profiled steel sheeting.

This work was financed by FEDER funds through the Competitivity Factors Operational Programme – COMPETE 2020 /Portugal 2020/UE within the scope of the research project POCI-01-0247-FEDER-003483.

References

Abas, F.M., Gilbert, R.I., Foster, S.J. and Bradford, M.A. (2013), "Strength and serviceability of continuous composite slabs with deep trapezoidal steel decking and steel fibre reinforced concrete", *Eng. Struct.*, **49**, 866–875. https://doi.org/10.1016/j.engstruct.2012.12.043.

Altoubat, S., Ousmane, H. and Barakat, S. (2015), "Effect of fibers and welded-wire reinforcements on the diaphragm behavior of composite deck slabs", *Steel Compos. Struct.*, **19**(1), 153-171. https://doi.org/10.12989/scs.2015.19.1.153.

Carmona, R.L., Branco, J.C. and Simões, R. (2009), "Lajes mistas com chapa colaborante: Soluções para melhorar o seu comportamento", In *VII Congresso de Construção Metálica e Mista* (pp. II-593-II–604). Lisbon, Portugal: CMM - Associação portuguesa de Construção Metálica e Mista.

CEN. (2002), EN 1990: Eurocode - Basis of structural design. Bruxelas: European Commitee for Standardization.

CEN. (2004a), EN 1992-1-1. Eurocode 2: Design of concrete structures - Part 1-1-: General rules and rules for buildings. Brussels: European Commitee for Standardization.

CEN. (2004b), EN 1994-1-1: Eurocode 4: Design of Composite Steel and Concrete Structures - Part 1-1: General Rules and Rules for Buildings. Brussels: European Commitee for Standardization.

CEN. (2006), EN 1993-1-3: Eurocode 3 - Design of steel structures; Part 1-3: General rules - Supplementary rules for cold-formed members and sheeting Eurocode. Brussels: European Commitee for Standardization.

Chen, S. (2003), "Load carrying capacity of composite slabs with various end constraints", *J. Constr. Steel Res.*, **59**(3), 385-403. https://doi.org/10.1016/S0143-974X(02)00034-2.

Chuan, D.L.Y., Abdullah, R. and Bakar, K.B. (2008), "Behaviour and load bearing capacity of composite slab enhanced with shear screws, **8**(6), 501-549.

Ferrer, M., Marimon, F. and Casafont, M. (2018), "An experimental investigation of a new perfect bond technology for composite slabs", *Constr. Build. Mater.*, **166,** 618-633. https://doi.org/10.1016/j.conbuildmat.2018.01.104.

Ferrer, M., Marimon, F. and Crisinel, M. (2006), "Designing cold-formed steel sheets for composite slabs: An experimentally validated FEM approach to slip failure mechanics", *Thin-Wall. Struct.*, **44**(12), 1261-1271. https://doi.org/10.1016/j.tws.2007.01.010.

Fonseca, A., Marques, B. and Simões, R. (2015), "Improvement of the behaviour of composite slabs : A new type of end anchorage", *Steel Compos. Struct.*, **19**(6), 1381-1402. https://doi.org/10.12989/scs.2015.19.6.1381.

ISO. (2009), ISO 6892-1. *Metallic Materials - Tensile Testing - Part 1: Method of Test at Room Temperature*. Switzerland.

Johnson, R.P. and Shepherd, A.J. (2013), "Resistance to longitudinal shear of composite slabs with longitudinal reinforcement", *J. Constr. Steel Res.*, **82**, 190-194. https://doi.org/10.1016/j.jcsr.2012.12.005.

Jolly, C.K. and Lawson, R.M. (1992), "End anchorage in composite slabs: an increased loadcarrying capacity", *Struct. Eng.*, **70**(11), 202-205.

Porter, M.L. and Greimann, L.F. (1984), "Shear-bond Strength of Studded Steel Deck Slabs", *Proceedings of the 7th International Specialty Conference on Cold-Formed Steel Structures*. St. Louis, Estados Unidos da América.

Rana, M.M., Uy, B. and Mirza, O. (2015), "Experimental and numerical study of end anchorage in composite slabs", *J. Constr. Steel Res.*, **115**, 372-386.

Salonikios, T.N., Sextos, A.G. and Kappos, A.J. (2012), "Tests on composite slabs and evaluation of relevant eurocode 4 provisions", *Steel Compos. Struct.*, **13**(6), 571-586. https://doi.org/10.12989/scs.2012.13.6.571.

Saravanan, M., Marimuthu, V., Prabha, P., Arul Jayachandran, S., and Datta, D. (2012), "Experimental investigations on composite slabs to evaluate longitudinal shear strength", *Steel Compos. Struct.*, **13**(5), 489-500. https://doi.org/10.12989/scs.2012.13.5.489.

Simões da Silva, L., Rebelo, C., Nethercot, D., Marques, L., Simões, R. and Real, P.M.M.V. (2009), "Statistical evaluation of the lateral – torsional buckling resistance of steel I-beams , Part 2 : Variability of steel properties", *J. Constr. Steel Res.*, **65**(4), 832-849. https://doi.org/10.1016/j.jcsr.2008.07.017.

Simões da Silva, L., Tankova, T., Marques, L. and Rebelo, C. (2018), "Safety assessment of EUROCODE 3 stability design rules for the lateral- torsional buckling of prismatic beams", *Adv. Steel Constr.*, **14**(4), 668-693. https://doi.org/10.18057/IJASC.2018.14.9.

Yang, Y., Liu, R., Huo, X., Zhou, X. and Roeder, C.W. (2018), "Static experiment on mechanical behavior of innovative flat steel plate-concrete composite slabs", *Int. J. Steel Struct.*, **18**(2), 473-485. https://doi.org/10.1007/s13296-018-0012-3.

CC